المجلة العلمية لجامعة الملك فيصل
The Scientific Journal of King Faisal University
العلوم الأساسية والتطبيقية
Basic and Applied Sciences

The Effect of Adding Nickel Content to Turbine Blades Coating Using Thermal Flame Spraying

Ashwaq T. Dahham[1], Sufian H. Humeedi[2], Salih Y. Darweesh[3], Ziad T. Khodair[4]

[1] Department of Physics, College of Science for woman, Baghdad University, Baghdad, Iraq
[2] Department of Physics, College of Science, Tikrit University, Tikrit, Iraq
[3] Physics Department, College of Education TuzKhurmatu, Tikrit University, Tikrit, Iraq
[4] Physics Department, College of Science, University of Diyala, Baqubah, Iraq

تأثير اضافة محتوى النيكل إلى طلاء الريش التوربينية بطريقة الرش الحراري

اشواق طارق دحام[1] و سفيان حواس حميدي[2] و صالح يونس درويش[3] و زياد طارق خضير[4]

[1] قسم الفيزياء، كلية العلوم للبنات، جامعة بغداد، العراق
[2] قسم الفيزياء، كلية العلوم، جامعة تكريت، تكريت، العراق
[3] قسم الفيزياء، كلية التربية طوزخورماتو، جامعة تكريت، تكريت، العراق
[4] قسم الفيزياء، كلية العلوم، جامعة ديالى، بعقوبة، العراق

KEYWORDS
الكلمات المفتاحية
Adhesion strength, cermet composites, hardness, porosity, thermal treatment
حيود الاشعة السينية، الصلادة، قوة التلاصق، المتراكبات السيرمتية، المسامية، المعاملة الحرارية

RECEIVED الاستقبال	ACCEPTED القبول	PUBLISHED النشر
11/06/2020	01/10/2020	01/12/2020

https://doi.org/10.37575/b/sci/2413

ABSTRACT

The current study dealt with manufacturing cermet composites from ceramic material (MgO) reinforced by a bonding nickel metal with different contents (0, 10, 15, 20, 25%) using thermal spraying by flame on steel surfaces (316L) with a constant spraying distance (15cm). The bases were cut into small circular shapes and roughened so that the coating layer was merged with them. The prepared samples were sintered at 800°C, 1000°C and 1200°C for two hours. Hardness, porosity, adhesion strength with different nickel contents, scanning by electron microscope (SEM) and X-ray diffraction (XRD) were tested. The test results revealed that nickel content of 20%, spraying angle of 90°, spraying distance 15cm and sintering at 1200°C gave good physical and mechanical properties. The SEM results also gave clear value in terms of surface topography and the grain's homogeneity with the best improvement at 1200°C. The best results for hardness and adhesion strength occurred at the nickel content of 20% accompanied by the lowest value of porosity at the same content. However, the results of XRD only showed that the material used was MgO with reinforcement material (Ni), which appeared in the Cubic phase.

الملخص

يتناول البحث الحالي تصنيع مواد سيرميتية بطريقة الرش الحراري باللهب من مادة سيراميكية (MgO) مدعمة بمادة رابطة معدنية النيكل وبنسب تدعيم مختلفة % (0, 10, 15, 20, 25), على قواعد من الفولاذ 316Lوبمسافة رش ثابتة((15cm, حيث تم تقطيع القاعدة الى قطع دائرية صغيرة وتم تخشينها لتكون اكثر اندماج مع مواد الطلاء، وتمت عملية التلبيد للعينات المحضرة عند 1200°C,1000°C,800°C ولزمن ساعتين فقط. اجريت اختبارات الصلادة والمسامية وقوة التلاصق مع محتوى النيكل المختلفة، وكذلك فحص المجهر الالكتروني الماسح (SEM), وفحص حيود الاشعة السينية (XRD). اظهرت نتائج الاختبار ان نسبة الخلط 20%وزاوية رش °90 ومسافة رش 15 cm وتلبيد بدرجة حرارة 1200°C تعطي خصائص فيزيائية وميكانيكية جيدة. اما نتائج مجهر(SEM) فقد اعطى ايضاً نتائج ذات قيمة واضحة من حيث طوبوغرافية السطح وتجانس الحبيبات كانت افضلها تحسن هي عند 1200°C, اما نتائج الصلادة وقوة التلاصق بلغت اعلاها عن نسبة الخلط % 20والتي رافقتها اقل قيمة من المسامية وعند نفس نسبة الخلط المثالية، أما نتائج حيود الاشعة السينية (XRD)فقط بينت ان المادة المستخدمة هي من الاساس (MgO) ومن مادة التدعيم النيكل (Ni) واللتان ظهرتا بالطور (Cubic).

1. Introduction

Composites are defined as materials produced by synthesizing two or more phases, producing high properties which include an increase in strength and reduction in weight. Consequently, there is a tendency towards producing composites to replace traditional engineering materials such as metals, alloys, polymers and ceramics (Kishawy *et al.*, 2019). The properties of composites are influenced by the properties of their constituent materials, which include a matrix and reinforcing phase, as well as the interface formed between phases and matrix. Matrix represents the continuous phase in composite, working to bond the elements and materials of reinforcement and connect the parts together to form a coherent synthetic system that can tolerate external forces (Pandi *et al.*, 2020). The reinforcement materials could be ceramic, metal or polymer to strengthen the matrix, and can be in the form of fibres, crusts or powders (Mu *et al.*, 2018). The reinforcement material employed in this study is nickel, which is widely used in manufacturing alloys, gas turbines and jet engine sections (Sharma *et al.*, 2020).

Composites are classified by type of matrix: metal matrix composites (MMCs), polymer matrix composites (PMCs) and ceramic matrix composites (CMCs) (Kalra *et al.*, 2018). In general, improving the properties of composites depends mainly on their manufacturing methods, whether by casting, powder technology or coating. Hence, the manufacturing method greatly affects the parameters of microstructure and will, therefore, affect the physical and mechanical properties of composites. Composites consisting of ceramic oxides with high melting degrees and elements such as magnesium, yatrium, aluminum and zirconium with the additions of ferrous materials are called Cermets. Recently, scientists have made a great effort to widely use these synthesized materials in various electrical and thermal applications that require good thermal insulation properties at high temperature ranges. This is attributed to their good thermal shocks resistance without any deformation under the thermal conditions used. Cermet composites are used as thermal barrier coatings in gas turbines, along with aircraft engines and naval engines (Rashed *et al.*. 2016; Smes *et al.*, 2016; Bourell *et al.*, 2017).

These materials also protect the metal base from oxidation, as in the exhaust silencer (Fauchais *et al.*, 2014). They are used in manufacturing braking discs in cars that are made of hard material, such as silica, mostly immersed in the plastic matrix phase of metal or bronze alloy. Additionally, cermet composites are used in ceramic transport engines, as the usefulness of all ceramic engines is illustrated by the low weight and high working rates that produce high efficiency (Michal *et al.*, 2002). Thus, the current research aims to investigate the possibility of activating the utilization of nickel and its properties in treating cracks on the turbine blades caused by exposure to high steam in large electric power plants or in places where the turbine blades are exposed to high temperatures.

Corresponding Author: Salih Y. Darweesh salih.younis@tu.edu.iq ,009647703978848 المؤلف المراسل: صالح يونس درويش

2. Materials and Methods

2.1. Materials Used and Preparation of Samples:

The coating base samples were selected from stainless steel of 316L type, and the alloy was cut into circular discs with a diameter of 20 mm and a thickness of 3mm. The matrix used contained magnesium oxide manufactured by Amdry Co. with a grain size of 63μm and a bonding nickel material with a grain size of 53μm of Indian origin from Himedia Co. was used. Cermet composites (Ceramic + metal) were prepared by taking different contents of (0, 10, 15, 20, 25%) from the bonding nickel material after a series of experiments and adding them to the matrix (MgO). The mixture was then stirred for two hours with an electric stirrer. After that, an initial thermal treatment of cermet composite powder was performed prior to coating at 100°C for 30minutes using a German-origin electric oven with a thermostat. The coating bases they were STAL Steel of 316L type, and they were cut and ground to the required dimensions for the samples holder and washed with alcohol to remove lubricants. A grit blasting tool manufactured by Sabtux Swedish Co. was used to increase the surface coarseness of samples. Grains used for coarseness were silicon carbide with diameters ranging from 0.7 mm - 1.6 mm. The coating bases were prepared for the spraying process, which used thermal spraying by flame. This method was used to coat all the prepared samples under study. Table (1) shows the elemental analysis for base coating (316L) and table (2) clarifies the parameters of the spraying process.

Table (1): Elemental analysis for base coating stainless steel (316L)

Elements	The ratio%
C	<0.03
Si	<1.00
Mn	<2.00
P	= <0.04
S	= <0.03
Cr	17.00
Mo	2.25
Ni	12.00
Fe	Remain

Table (2): parameters of thermal spraying process

Oxy-acetylene Mixing	3:1
Coating time	(2 min)
Maximum thickness coating	(1-1.5)mm
Rotation number	4
Particle size of powders	(53-63)μm
Flame spraying temp.	3000°C
Spraying distance	15cm
Concentration of nickel	(0, 10, 15, 20, 25) %
Sintering	(800, 1000, 1200)°C

2.2 Examinations and Measurements:

2.2.1. Scanning Electron Microscope (SEM)

The samples were examined using TESCAN type Vega III model SEM of Czech-origin. The SEM gives a detailed 3D and magnified image. The samples to be examined were placed in a column free of air in the electron microscope through an opening or sealed tap as the samples were coated with silver or gold to have electrical conductivity.

2.2.2. X-Ray Diffraction Test

An x-ray is an electromagnetic radiation with a very short single wavelength ranging from 0.25 to 0.5 angstrom, and it has a light-like nature, but with a shorter wavelength. It is produced by striking electrons with the target metal inside the x-ray tube. The English scientist W. L. Bragg found a mathematical equation to determine the distance between crystal levels through x-ray diffraction. He used the principle that x-rays are scattering inside the crystal in all directions when falling on the crystal. Therefore, the phases formed by the material and the material type were defined by applying the following equation (Derwesh *et al.*, 2019):

$$2d\,\mathrm{Sin}\theta = n\lambda \quad \text{.....(1)}$$

Where (d) refers to the spacing between diffracting planes, (θ) is the diffraction angle (Bragg angle, half the angle between the angle of incidence and angle of refraction), (λ) is the wavelength (1.5418 Å) and (n) is an integer. The X-ray diffraction of compacts was examined using a Japanese-origin XRD-6000 SHIMADZU device. The tube used was (Cu) kα. Tests were conducted at room temperature.

2.2.3. Hardness Test

The Vickers hardness test can be performed by creating a small indentation using a square-based diamond pyramid indenter. This indentation is a result of forcing a load on the material surface. In this test, hardness values were determined by measuring the size of the pyramidal gap by applying the following equation (Darweesh *et al.*, 2019):

$$Hv=1.8544\ P/D^2_v\ (Kg/mm^2) \quad \text{..... (2)}$$

Where (P) is the load applied (Kg) and (D_v) is the average length of the diagonal left by the pyramidal indenter resulting from applying the load on the surface (mm). Figures 2-11 show the Vickers hardness test and the extent of angles between the surfaces. The ten readings of the compressed sample (five readings for each side of the compression) were recorded radially from the centre of the compression surface to its boundary, and the average of those readings was calculated.

2.2.4. Porosity Test

A porosity test was performed using the samples of coating layer after removing it from the surface during the examination. Archimedes' principle of immersion was used to calculate the proportion of pores in accordance with standard specifications (ASTM-C830) (Darwish et al 2020). Hence, the sample was weighed as dry (W_1) using an electrical balance of (±0.0001 gram). To achieve this, an electric oven was used to dry the samples for half an hour. Then, the samples were placed in a container full of distilled water, and the container was emptied from the air using a rotary pump. The appearance of air bubbles was observed in the water, and they disappeared when the container was opened. The sample was then taken out and excess water was wiped from its surface using a wet cotton cloth, taking care not to remove water from the pores. The sample was weighed again (W_2). Finally, the sample was weighed as submerged in water (W_3), and porosity (%P°) was calculated using the following equation (C830 1988):

$$P\% = (W_2\text{-}W_1/\ W_2\text{-}W_3)\times 100 \quad \text{..... (3)}$$

2.2.5. Adhesion Test

An adhesion test on the coating layer was performed using a tensile tool of the Microcomputer Controlled Electronic Universal Testing Machine (WDW-50E) manufactured by the German Time Group Inc. according to specifications (ASTM A370). The adhesion samples (the sprayed and unsprayed samples) were installed between the jaws of the tensile tool after sticking them together using epoxy adhesive. This was done by putting a thin adhesive layer on the coating surface so that it covered all surface parts, ensuring that it was regular, then, the two samples were compacted together for one hour and placed in a drying oven for 24hour at 50 °C. After installing the samples in the tool, a tensile load was applied to each test sample at a rate of 1mm/min until the sample failed. Hence, the maximum load applied was recorded and the adhesion strength was calculated using this equation (Darweesh *et al.* 2019, Dahham et al.

2020):

Adhesion strength = maximum Load/ cross Section = F/A..... (4)

2.2.6. Spray Angle

In thermal spraying by flame, the preferred angle is 90°. Even when the spray angle reaches 45°, it does not have a noticeable effect on the coating composition. When the angle is below 45°, it affects the coating composition ,which is called shadow effect. A shadow effect results from blocking the droplets' course by the coating surface formed (Matikainan *et al.*, 2014).

3. Results and Discussion

3.1. SEM Results:

The study of the topography of coatings' surfaces is important in understanding the cohesion and distribution of the reinforced material on the surface of the substrate and the method of fusion that improves the properties in general, and to identify the differences and the characteristics' homogeneity of each sample. Electronic images of the samples were taken at the best distance found (15cm) before and after the thermal treatment of the samples. Figure (1-a) illustrates an SEM image of magnesia powder (matrix) at (1µm), the type of powder used and the size of its component atoms, Figure (1-b) shows the reinforcement bonding material (nickel) and how the atoms are arranged together.

Figure 1: an SEM image for (a) Magnesia powder (MgO), (b) Nickel powder (Ni).

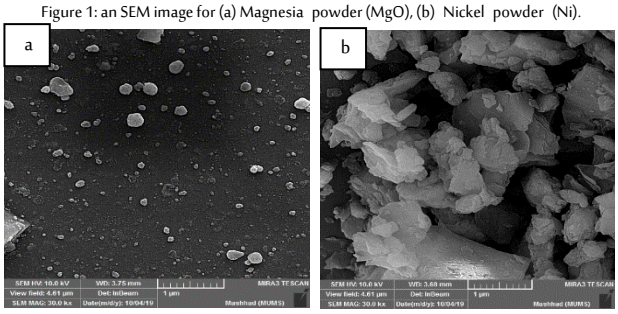

Figure (2) clarifies the SEM images of cermet composite at (50µm) for all samples prepared after thermal treatment and coating process. It is observed that figure (2-a) presents an image of a sample coated without sintering, showing the characteristics of the coated powders distinctly and the grains' cohesion to each other. Figure (2-b) gives a cross-section image after thermal treatment and sintering at (800 °C). It indicates a homogeneous but rather random bond between composite components with a clear thermal effect through grains' cohesion and the spread of some surface defects with pores in the microstructure (Xiang *et al.* 2001). Also, there are low-density and high-density areas, resulting in elements' separation and inhomogeneity. As for figure (2-c) at thermal treatment (1000°C), it is observed that the lateral-section microstructure is more homogenous with a stronger and greater bond as a result of cermet material grains' integration with their components due to high and effective temperatures. Additionally, there is interaction between particles for both powders with obvious pores in the sample surface. In figure (2-d) at thermal treatment (1200 °C), there is a great homogeneity between the cermet components of ceramics and metal where the strength of homogeneity and cohesion has a great effect by reducing porosity and increasing hardness (Darweesh *et al.* 2019). This figure shows a semi-full symmetry among grains which became smaller. Hence, sintering at this degree is the best in terms of improving the mechanical and physical properties of samples prepared by this technique.

Figure 2: SEM images for samples prepared after coating (a) at room temperature (R.T), (b) at 800°C, (c) at 1000 °C and (d) at 1200 °C

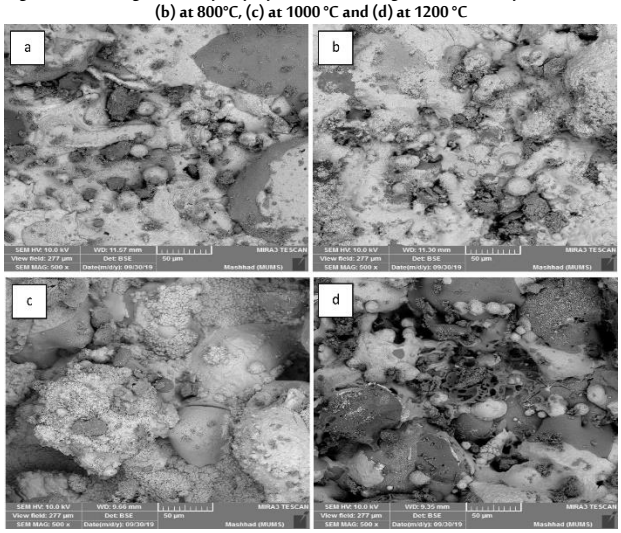

3.2. Hardness Results:

The effect of spray distance on the mechanical hardness values of the cermet coating layers before thermal treatment is shown in figure (3). It is observed that, at low reinforcement values, hardness is low due to high porosity at these distances and the low nickel content has a significant effect on filling the pores. But, after increasing nickel content to 20%, the hardness value is high with minimum porosity. After increasing the content, the hardness values begin to decrease gradually due to the decrease in the bonding strength of coating and the increase in porosity. When performing thermal treatment at 1200 °C for two hours, the hardness values become higher as clarified in figure (4), due to the low percentage of pores. This, in turn, improves the properties of the coating layer due to sintering and diffusion, which leads to increasing the bonding strength between the cermet coating layer and matrix (Darweesh *et al.*, 2019).

Figure 3: hardness with nickel content before thermal treatment.

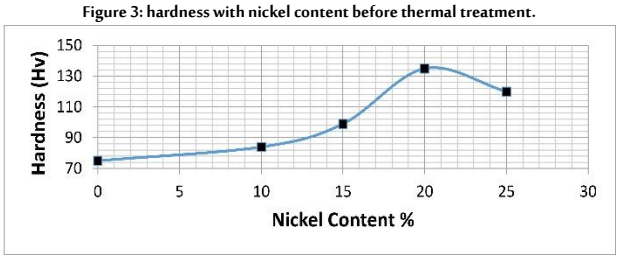

Figure 4: hardness with nickel content after thermal treatment at 1200°C for two hours.

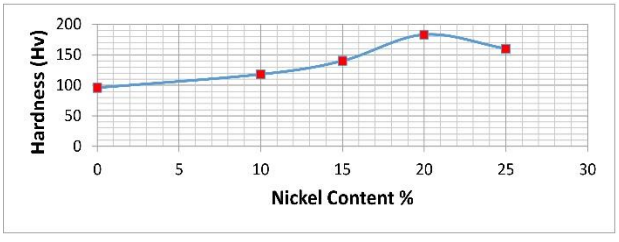

3.3. Porosity Results:

Figure (5) illustrates the effect of spray distance on the porosity percentage of the coating layer of the cermet composite before thermal treatment. It is found that using low reinforcement content gives high porosity value of the layer produced and this value decreases gradually with the increase in reinforcement content to 20% and increases again with increasing nickel to 25%. The reason

for the increase in porosity when using low reinforcement content may be attributed to the inability of molten droplets to fully flatten and correlate with other droplets due to the high cooling rate which results from withdrawing heat to the base. Therefore, the droplets will suffer from thermal shrinkage after their solidification (Sameen *et al.* 2018). As for the contents greater than 20%, it is also observed that there is an increase in porosity because the drops are relatively cold and have less velocity and kinetic energy. Therefore, the layer will be an asymmetric aggregation with the possibility of partial solidification of drops before striking the surface, leading to their poor adhesion. When performing thermal treatment on the cermet coating layers, it is observed that the porosity percentage is lower than that before thermal treatment as described in figure (6). This means that thermal treatment leads to atoms diffusing sufficiently to form new bonding areas between the layers through the movement of atoms between them attempting to close the pores (Darweesh *et al.*, 2019).

Figure 5: Porosity with spray distance before thermal treatment

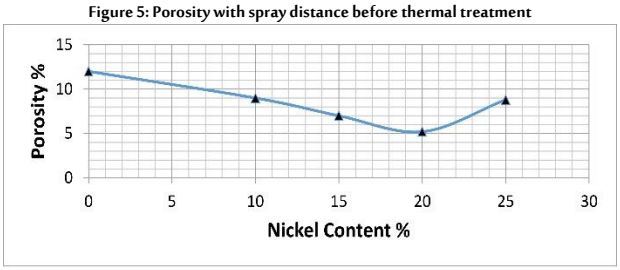

Figure 6: Porosity with spray distance after thermal treatment at (1200 °C) for two hours .

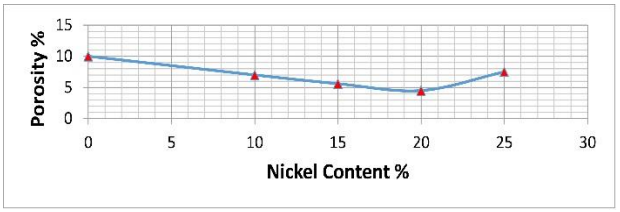

3.4. Adhesion Strength Results:

Figures (7) and (8) illustrate the relationship between nickel content and adhesion strength before and after thermal treatment at 1200 °C. It is observed that, after thermal treatment, adhesion strength is greater due to high hardness and the intensity of the coating layer using thermal spray. The increase in nickel content leads to greater adhesion strength between the surface and coating layer. With 25% nickel content, adhesion strength is reduced due to the drop in molten temperature, which in turn increases the liquid phase. The droplets have high enough velocity to cause plastic deformation when striking the surface. This leads to a decrease in the molten particle's ability to form an adhesive layer with it. Surface, but, with less than 20% nickel content, adhesion strength is high because of low porosity (Planche *et al.*, 2005).

Figure 7: Adhesion force with nickel content before thermal treatment

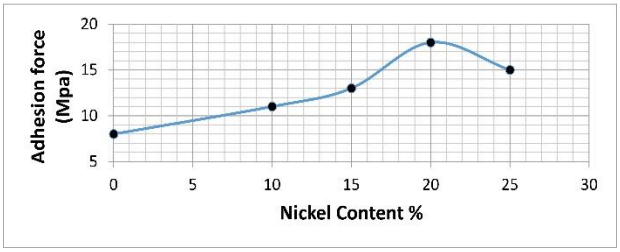

Figure 8: adhesion force with nickel content after thermal treatment at 1200 °C for two hours .

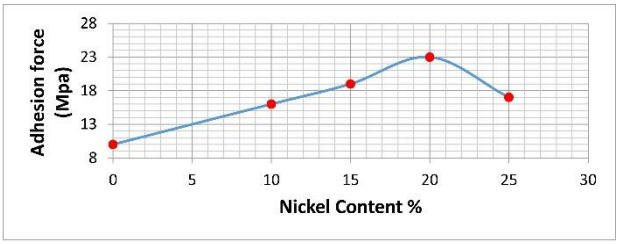

3.5. Effect of Spray Angle on Porosity and Hardness of the Cermet Coating Layer:

Various spray angles (30°,45°,50°,75°,90°) were selected to observe the effect of changing these angles on the porosity and hardness of thermal spray coatings at a constant spray distance (15cm) and thermal treatment (1200°C) with a nickel content of 20%. Figure (9) shows that at a low angle (30°), porosity is high and the course of droplets striking the coating surface does not fully cover all of its area. This effect leads to the formation of an inhomogeneous surface with a porous structure where mechanical properties, such as hardness and adhesion resistance, are reduced. When increasing the spray angle (45°), the percentage of pores begins to decrease due to the effect of the microstructure of coating layers on the spray angle. Hence, the change of the spray angle controls the flow of the molten coating material. It is found that the porosity values are lowest when the spray angle is 90°, i.e., vertically towards the base surface where all molten droplets fill the base surface, forming a thick coating layer free of surface defects. This is consistent with figure (10) which shows that the increase in hardness of the cermet coating layers is caused by increasing spray angles. In addition, an angle of 90° produces coating layers with a high hardness that are coherent, homogeneous and almost free of surface defects (Xie *et al.*, 2019).

Figure 9: Effect of spray angles on porosity

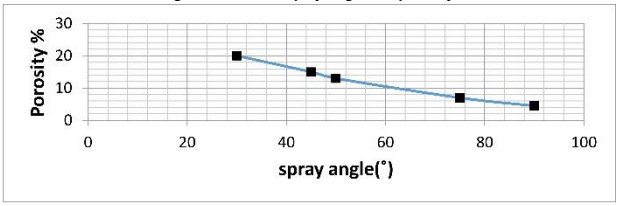

Figure 10: Effect of spray angles on hardness

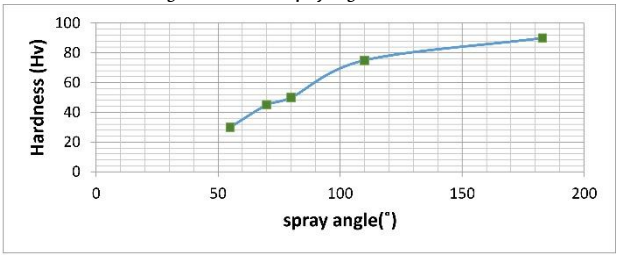

3.6. XRD Results:

Figure (11) clarifies the XRD results of the cermet coating material (MgO-20%Ni). Figure (12-a) represents XRD after coating at room temperature (R.T); while figure (12-b) shows XRD after thermal treatment at 800°C where the matrix is clear as (MgO) at the five angles (2θ = 37.296, 43.284, 62.936, 75.436, 79.418). Whereas nickel reinforcement material (Ni) is located at the three angles (2θ = 44.534, 51.889, 76.395). Figures (12-c and d) represent the

composite after thermal treatment at 1000°C and 1200°C, respectively, which shows that the phase formed is cubic. According to the card numbers (96-900-6816) and (96-901-3025) (Suh *et al.* 1988, Zhang 2000), nickel is in a clear crystalline phase with magnesia with a rise in peaks and the amount of sintering. This in turn improves the properties of the prepared samples significantly.

Figure 11: X-ray diffraction of (MgO-20%Ni) system at different thermal treatments (a) at room temperature (R.T), (b) at 800 °C, (c) at 1000 °C, (d) at 1200 °C.

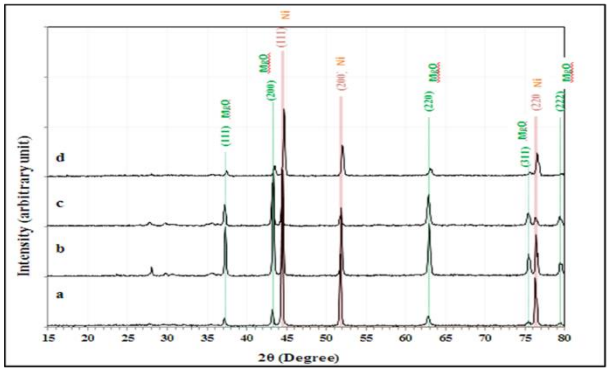

4. Conclusion

This study concluded that, when using thermal spraying by flame for coating the cermet material (MgO-Ni), the best parameters affecting the properties of the cermet coating layer were observed at a spray distance of 15cm, spray angle of 90°, thermal treatment of 1200 °C for two hours and reinforcement content 20%. These parameters gave the highest hardness value (183 Hv), the lowest porosity (4.5%) and the highest adhesion strength (23Mpa) for the coating layer. Regarding the SEM result, it gave a clear surface topography characterized by homogeneity and clarity of coherent grain boundaries (50μm). Also, x-rays diffraction demonstrated the appearance of both matrix and reinforcement material at the cubic crystal phase at the same ideal coating conditions previously mentioned. With simple conditions, such as measuring devices for hardness, porosity, a scanning electron microscope and x-ray diffraction, it is possible to create models that help solve the problem of cracks and damages occurring on turbine blades. This, in turn, helps to extend the service life of turbine blades.

Bios

Ashwaq T. Dahham

Physics Department, College of Science for Woman, Baghdad University, Baghdad, Iraq, 009647500131896, ashwaqtariq@yahoo.com

Works as a teaching doctor at the College of Science, University of Baghdad. After obtaining a bachelor's degree from the College of Science in 2001, she was one of the first to work as a teaching assistant in her college. She also obtained a master's degree at the College of Science in 2009. After that, she completed her PhD in solids and materials in 2018, Jurisdiction/Solids and Materials Physics.

Sufian H. Humeedi

Physics Department, College of Science, Tikrit University, Tikrit, Iraq, 009647702797851, sufianhh@yahoo.com

Holds a master's degree from 2004. Academic title: history teacher, having obtained the title of history teacher in 2011. Has attended many local and international seminars in the field of physics, as well publishing a number of research paper Locally and globally.

Salih Y. Darweesh

Physics Department, College of Education, Tikrit University, Tuzkormato, Iraq, 009647703978848, salih.younis@tu.edu.iq

Obtained a bachelor's degree in physics from the University of Mosul, Iraq 2012, a master's degree in physics from Tikrit University, Iraq 2014 and a doctoral degree in physics from Tikrit University, Iraq 2018. He has also had many papers published within scopes containers as well as at the local level. The researcher has also participated in many conferences, both inside and outside the country. Current position is the head of the physics department at the College of Education, Tuzkormato, Tikrit University, Iraq.

Ziad T. Khodair

Physics Department, College of Science, University of Diyala, Baqubah, Iraq, 009647703409844, ziad_tariq70@yahoo.com

Authored more than 40 scientific publications and has been a member of many committees and organisational bodies. He obtained his BSc in Physics from Al-Mustansiriya University 1992 and his MSc in thin films physics in 2003. He also obtained his PhD in Physics/Nanomaterials from University of Baghdad in 2011. He worked as the head of the physics department. He has taught many postgraduate and undergraduate subjects including solid state physics.

References

Bourell, D., Kruth, J. P., Leu, M., Levy, G., Rosen, D., Beese, A. M. and Clare, A. (2017). Materials for Additive Manufacturing. *CIRP Annals*, **66**(2), 65981.

Dahham, A. T., Darweesh, S. Y. and Jassim, I. K. (2020). Structural and Thermal Unusual Properties in Invar and Behaviour of Ni-Mn Alloys. *Baghdad Science Journal*, **17**(2 Special Issue NICST), 629–32.

Darweesh, S. Y., Ali, A. M., Khodair, Z. T. and Majeed, Z. N. (2019). The Effect of Some Physical and Mechanical Properties of Cermet Coating on Petroleum Pipes Prepared by Thermal Spray Method. *Journal of Failure Analysis and Prevention*, **19**(6), 1726–38.

Darweesh, S. Y., Jassim, I. K. and Mahmood, A. S. (2019, September). Characterization of Cerment composite coating Al2O3-Ni system. *Journal of Physics: Conference Series*, **1294**(2), 022011.

Darwish, S. Y. and Majid, Z. N. (2020). Improving the durability of streak and thermal insulation of petroleum pipes by using polymeric based paint system. *Baghdad Science Journal*, **17**(3), 826.

Fauchais, P. L., Heberlein, J. V. and Boulos, M. I. (2014). Industrial Applications of Thermal Spraying Technology. *Thermal Spray Fundamentals*, **n/a**(n/a), 1401–6.

Hussein, I. F. (2017). Study of the physical and morphological properties of ceramic insulator. *Ibn AL-Haitham Journal for Pure and Applied Science*, **23**(3), 1–9.

Kalra, C., Tiwari, S., Sapra, A., Mahajan, S. and Gupta, P. (2018). Processing and Characterization of Hybrid Metal Matrix Composites. *Journal of Materials and Environmental Science*, **9**(7), 1979–86.

Kishawy, H. A. and Hosseini, A. (2019). Metal Matrix Composites. *Machining Difficult-to-Cut Materials*, **n/a**(n/a), 139–77.

Matikainen, V., Niemi, K., Koivuluoto, H. and Vuoristo, P. (2014). Abrasion, Erosion and Cavitation-Erosion Wear Properties of Thermally Sprayed Alumina Based Coatings. *Coatings*, **4**(1), 18–36.

Mohammed, S. F. and Darweesh, S. Y. (2018). Effect of thermal treatment on some physical and mechanical properties of cermet coating by flame spraying technology. *Journal of University of Babylon for Pure and Applied Sciences*, **26**(7), 269–80.

Mu, T., Liu, L., Lan, X., Liu, Y. and Leng, J. (2018). Shape Memory Polymers

for Composites. *Composites Science and Technology*, **160**(26), 169–98.

Pitchai, P., Berger, H. and Guruprasad, P. J. (2020). Investigating the Influence of Interface in a Three-Phase Composite Using Variational Asymptotic Method-Based Homogenization Technique. *Composite Structures*, **233**(1), 111562.

Planche, M. P., Liao, H., Normand, B. and Coddet, C. (2005). Relationships Between NiCrBSi Particle Characteristics and Corresponding Coating Properties Using Different Thermal Spraying Processes. *Surface and Coatings Technology*, **200**(7), 2465–73.

Rashed, M. G., Ashraf, M., Mines, R. A. W. and Hazell, P. J. (2016). Metallic Microlattice Materials: A Current State of the Art on Manufacturing, Mechanical Properties and Applications. *Materials & Design*, **95**(5), 518–33.

Sames, W. J., List, F. A., Pannala, S., Dehoff, R. R. and Babu, S. S. (2016). The metallurgy and processing science of metal additive manufacturing. *International Materials Reviews*, **61**(5), 315–60.

Sharma, A. K., Bhandari, R., Aherwar, A. and Rimašauskienė, R. (2020). Matrix Materials Used in Composites: A Comprehensive Study. *Materials Today: Proceedings*, **21**(3), 1559–62.

Suh, I. K., Ohta, H. and Waseda, Y. (1988). High-Temperature Thermal Expansion of Six Metallic Elements Measured by Dilatation Method and X-ray Diffraction. *Journal of Materials Science*, **23**(2), 757–60.

Xiang, Y., Hu, W., Liu, X., Zhao, C. and Ding, W. (2001). Initial Deposition Mechanism of Electroless Nickel Plating on Magnesium Alloys. *Transactions of the IMF*, **79**(1), 30–2.

Xie, K., Qiu, X., Cui, Y. and Wang, J. (2020). Experimental Study on the Effect of Spray Cone Angle on the Characteristics of Horizontal Jet Spray Flame Under Sub-Atmospheric Pressure. *Thermal Science*, **24**(5A), 2941–52.

Zhang, J. (2000). Effect of Pressure on the Thermal Expansion of MgO up to 8.2 GPa. *Physics and Chemistry of Minerals*, **27**(3), 145–8.